Spectrochimica Acta Part A: Molecular and Biomolecular Spectroscopy 239 (2020) 118457

Contents lists available at ScienceDirect

Spectrochimica Acta Part A: Molecular and Biomolecular Spectroscopy

journal homepage: www.elsevier.com/locate/saa

Chromogenic detection of hydrogen sulfide using squarylium-based chemosensors

Ha Lim Noh [a,1], Byeong M. Oh [a,1], Young Ki Park [b], Hye W. Chun [a], Junyeop Lee [c], Jae Keon Kim [c], Jian Zheng [a,d], Daewoong Jung [c,*], Woosung Lee [b,*], Jong H. Kim [a,*]

[a] Department of Molecular Science and Technology, Ajou University, Suwon 443-749, Republic of Korea
[b] Smart Textiles R&D Group, Korea Institute of Industrial Technology (KITECH), 143 Hanggaulro, Sangnogu, Ansan-si, Gyeonggi-do 426-910, Republic of Korea
[c] AI System Technology Group, Korea Institute of Industrial Technology (KITECH), Daegu 41566, Republic of Korea
[d] School of Chemistry and Chemical Engineering, Lingnan Normal University, Zhanjiang, China

ARTICLE INFO

Article history:
Received 3 February 2020
Received in revised form 22 April 2020
Accepted 6 May 2020
Available online 08 May 2020

Keywords:
Spectroscopic characterization
Colorimetric chemosensor
Squarylium derivative
Hydrogen sulfide
Selectivity

ABSTRACT

Squarylium-based colorimetric hydrogen sulfide (H_2S) chemosensors (SQ1, SQ2, and SQ3) were developed, and their detection properties were systematically characterized. SQ1 exhibited rapid and high resolution H_2S sensing properties through significant color changes detectable by naked-eye with limit of detection as low as 7.2 ppb. SQ1 also showed excellent selectivity for H_2S detection over other relevant anions and nucleophiles. Sensing mechanisms of SQ1 were investigated based on spectroscopic and ^1H NMR analyses with quantum calculations. Furthermore, SQ1 showed an efficient response to H2S under versatile conditions in the solution, solid, and dyed fabric states, which suggests applicability of SQ1 to simple, low-cost, and practical H_2S sensors.

1. Introduction

Hydrogen sulfide (H_2S) is a water-soluble and colorless gas with a bad order of rotten egg that is usually produced by the decomposition of organic compounds or from byproduct of farming, waste management, and petroleum refining [1]. H_2S has been regarded as an environmental pollutant due to its corrosive, toxic and detrimental effects, in particular damage to environment and biological systems of human bodies [2]. Abnormally high concentration of H_2S damages pipelines and catalysts and ceramic membranes used in syngas separations [3] or causes various diseases such as liver cirrhosis and Alzheimer's diseases [4]. Recently, with growing concerns on public safety and health care, precise detection of H_2S for environmental monitoring or medical diagnostic purposes has attracted significant attention in environmental and biological industry.

Traditional methods for the detection of colorless H_2S gas include gas chromatography (GC) [5], electrochemical analysis [6], and metal-induced sulfide precipitation [7], plasma-atomic emission [8], and surface-enhanced Raman scattering [9]. However, because these methods not only require extensive sample preparation and complexed, high-cost, and stationary instruments but also have low temporal resolution they are not compatible with rapid, portable and high-resolution detection. More recently, to overcome these limitations, fluorescent chemosensors have been developed for the detection of H_2S [10]. However, preparation of most of these fluorescent chemosensors possesses complexed and multi-step synthetic routes and observation of fluorescent emission change requires additional UV excitation light source, which impedes their feasibility. Thus, development of simple but highly sensitive naked-eye-based H_2S sensory system for the effective detection of H_2S is highly desirable for the practical applications. Squarylium dyes and derivatives are 1,3-disubstituted compounds which can be synthesized from one-step reaction between squaric acid and two equivalents of various types of electron donating moieties. A lot of efforts have been made to develop various squarylium derivatives due to the simple synthetic process and their appealing optical merits such as sharp and intense absorbance and fluorescence in the visible to near-infrared region. As a result, in recent years, squaraine dyes have been extensively used in optical data storage, solar cells, non-linear optics, and chemosensors [11]. Motivated by such simple synthetic process and unique optical properties of the squarylium dyes, we have turned our attention to the application of squarylium derivatives to the H_2S detection. In particular, we focused on the naked-

* Corresponding authors.
E-mail addresses: dwjung@kitech.re.kr (D. Jung), wslee@kitech.re.kr (W. Lee), jonghkim@ajou.ac.kr (J.H. Kim).
[1] These authors (Ha Lim Noh and Byeong M. Oh) contributed equally to this work.

https://doi.org/10.1016/j.saa.2020.118457
1386-1425/

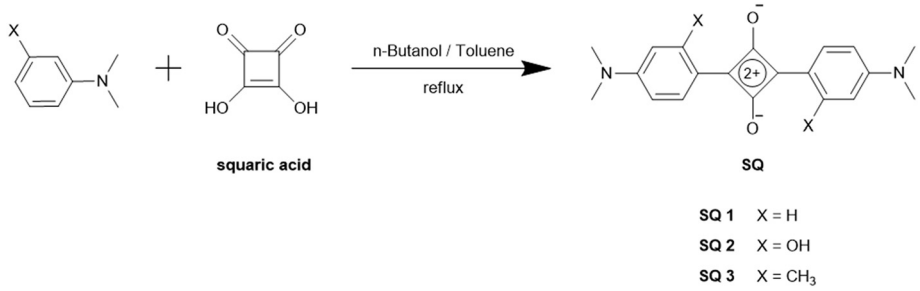

Scheme 1. Synthetic step for SQ dyes.

eye-based colorimetric changes of squarylium derivatives in response to H_2S. In this work, we developed three squarylium chemosensors (**SQ1**, **SQ2**, and **SQ3**) for the detection of H_2S, revealed sensing mechanism, and suggest principles for the efficient detection. More importantly, SQ1, showing excellent sensing resolution with a limit of detection as low as 0.211 μM, exhibited excellent colorimetric response to H_2S under versatile conditions including solution, solid sates and dyed textiles, which suggests practical application of **SQ1** to the H_2S sensors.

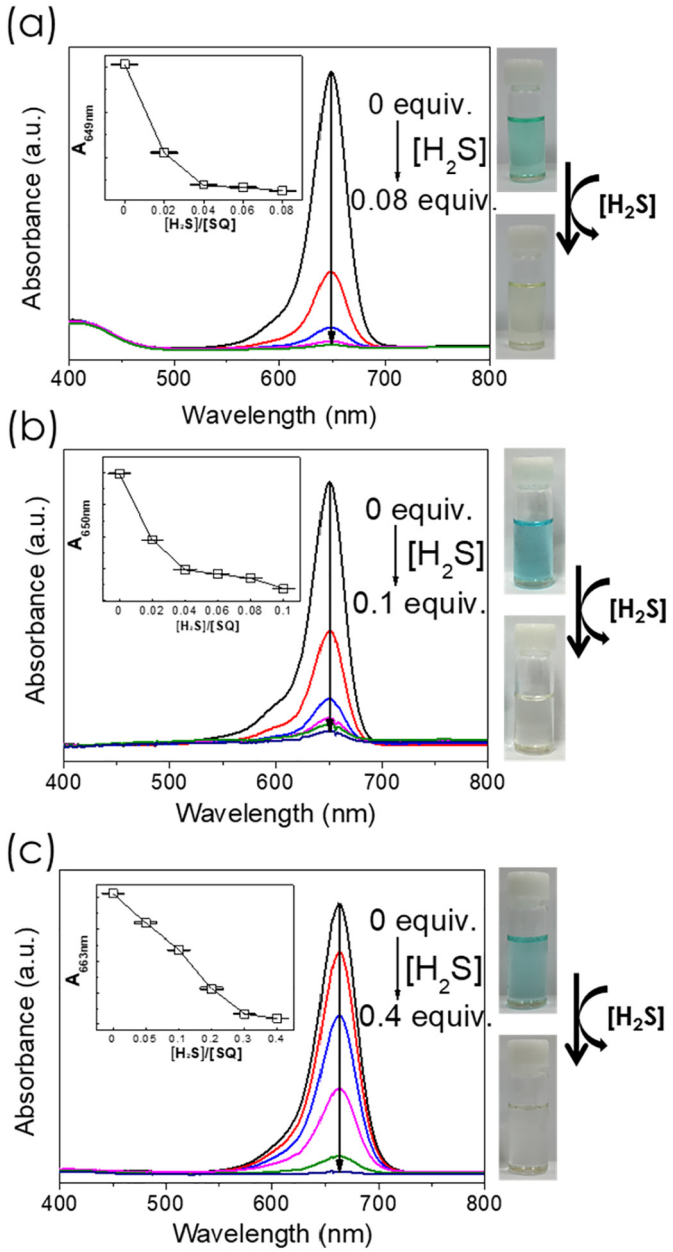

Fig. 1. Changes in UV–Vis absorption spectra for (a) **SQ1** (1.0×10^{-4} M), (b) **SQ2** (2.5×10^{-4} M), (c) **SQ3** (5.0×10^{-5} M) upon addition of H_2S. Insets are photographs of SQ dyes solutions showing color changes after H_2S addition.

2. Experimental section

2.1. Materials

All reagents and solvents were purchased from Sigma Aldrich and TCI and were used without further purification. H_2S solution was prepared by dissolution of NaSH in water. All titration and selectivity experiments in vitro were performed.

2.2. The synthesis of SQ1, SQ2 and SQ3

2.2.1. SQ1

Squaric acid 3 (0.343 g, 3 mmol) and *N*,*N*-dimethylaniline (0.727 g, 6 mmol) were heated under reflux for 12 h in a mixture of 20 ml of n-butanol/toluene (1: 1/v:v). The reaction mixture was cooled to room temperature. The precipitated crude products were separated by filtration and washed with n-hexane and methanol.

Yield 16%; ^{1}H NMR (600 MHz, $CDCl_3$) δ 3.22 (s, 12H), 6.81 (d, 4H), 8.43 (d, 4H); mp: 305 °C; LC-MS calcd *m*/*z*: 320.38, found 321.2 $[(M+1)]^+$.

The squarylium dyes SQ2 and SQ3 were obtained by a similar procedure using 3-(dimethylamino)phenol and *N*,*N*-dimethyl-m-toluidine, respectively.

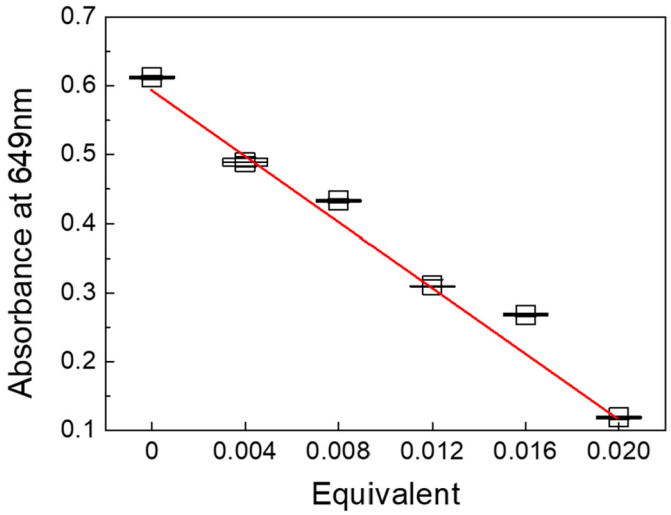

Fig. 2. Limit of detection measurement for **SQ1** to H_2S.

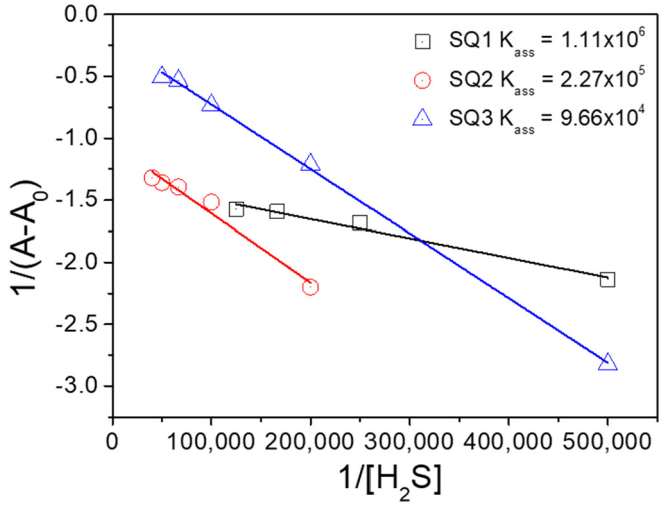

Fig. 3. Benesi-Hildebrand plots of **SQ1**, **SQ2** and **SQ3** with H_2S.

2.2.2. SQ2

Yield 92%; ^{1}H NMR (600 MHz, CD_2Cl_2) δ 3.16 (s, 12H), 6.14 (s, 2H), 6.41 (d, 2H), 7.86 (d, 2H); mp: 330 °C; LC-MS calcd *m/z*: 352.38, found 353.1 $[(M+1)]^+$.

2.2.3. SQ3

Yield 25%; ^{1}H NMR (600 MHz, CD_2Cl_2) δ 2.87 (s, 6H), 3.17 (s, 12H), 6.61 (m, 4H), 8.90 (d, 2H); mp: 280 °C; LC-MS calcd *m/z*: 348.44, found 349.3 $[(M+1)]^+$.

2.3. Characterization

An Electrothermal IA900 melting point apparatus was used to determine melting points. JEOL spectrometer was used to obtain the ^{1}H NMR spectra by using chloroform-*d* and DMSO-d_6. Agilent 8453 spectrophotometer was used to perform the spectral measurements of UV–Vis absorption. Fluorescence spectra were recorded by JASCO FP-8200 spectrofluorometer. UV–Vis absorption and fluorescence measurements were performed by the addition of analytes to the squarylium dye solution in 4:1 DMSO:H_2O at room temperature. The color parameters of the dyed PET fabric were obtained using a reflection spectrophotometer (Color-Eye 7000A).

3. Results and discussion

Symmetrical squarylium dyes (**SQ1**, **SQ2**, and **SQ3**) were synthesized using condensation of squaric acid (**2**) and electron rich units, *N*,*N*′-dimethylaniline, 3-(dimethylamino)phenol, and *N*,*N*′-dimethyl-*m*-toluidine (**1**) (Scheme 1). Detailed synthetic procedures are given in the Experimental section.

First, we carried out spectral studies by monitoring changes in shape of UV/Vis absorption of the synthesized SQ dyes to examine the feasibility for the colorimetric detection of H_2S. As shown in Fig. 1, solutions of SQ1, SQ2, and SQ3 exhibited sharp and intense absorption band (λ_{max}) at 649, 650, and 663 nm, respectively. Colorimetric responses to H_2S, produced from NaSH (a standard source for H_2S) [12], were observed for three dye solutions. As shown in Fig. 1, with addition of H_2S to 1.0×10^{-4}, 2.5×10^{-4}, 5.0×10^{-5} M of SQ1, SQ2, and SQ3 solutions, respectively, absorbance of three solutions were progressively decreased, accompanied by changes in the color of the solutions from light blue to colorless within 5.0 s. We note that SQ1 solution exhibited detection

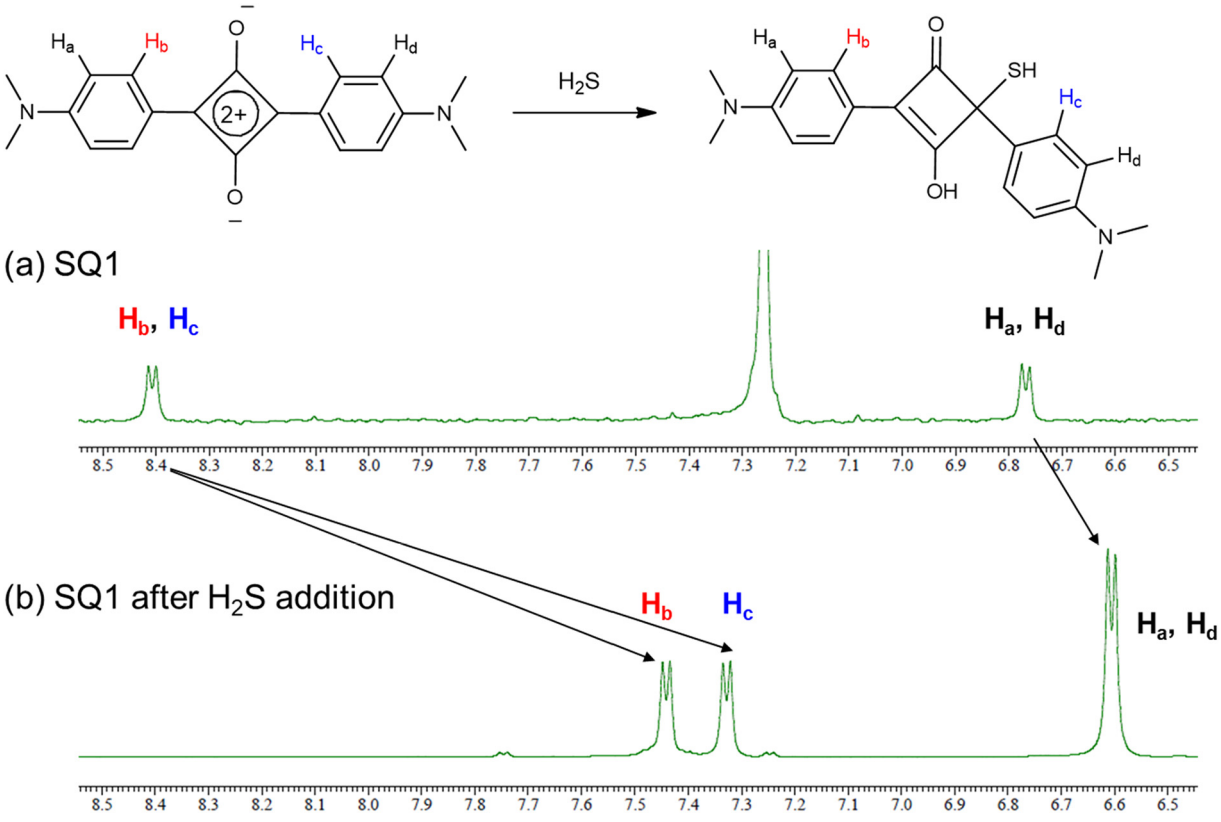

Fig. 4. ^{1}H NMR spectral change of **SQ1** in $CDCl_3$ and DMSO-d_6/H_2O (4:1, v/v) (a) before and (b) after addition of H_2S.

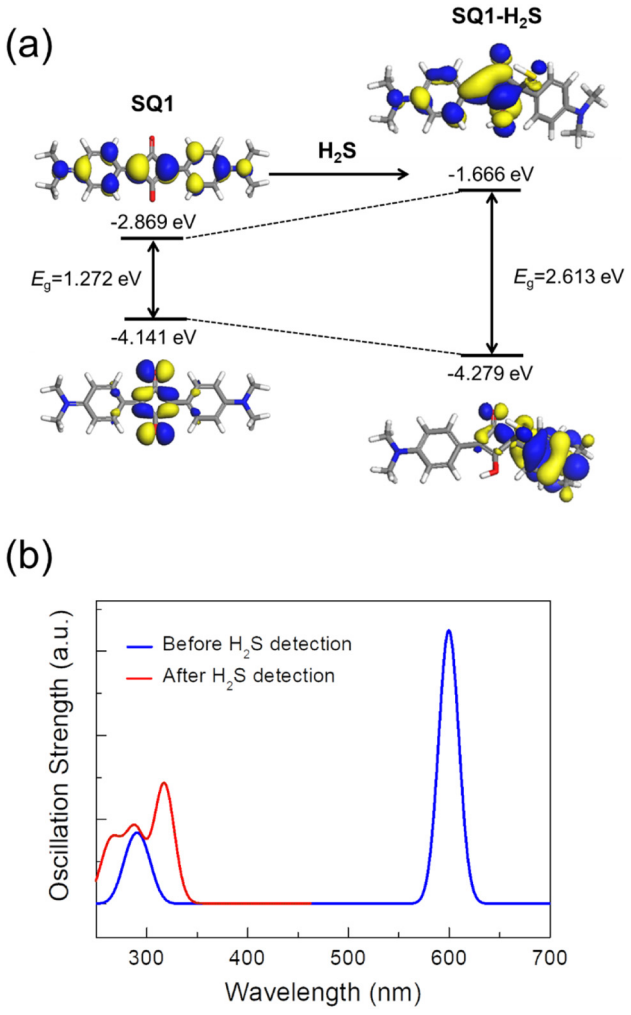

Fig. 5. (a) Electron distribution of the HOMO and LUMO energy levels and (b) calculated oscillator strength of **SQ1** before and after reaction with H_2S.

stability in different pH ranging from 3 to 9 (Fig. S2). Interestingly, it was found that reactivities or sensitivities of the three dyes are different. Absorption band at λ_{max} of SQ1 exhibited completely disappeared with 0.08 equivalent (8.0 μM) of H_2S while those for SQ2 and SQ3 were observed at 0.1 equivalent (20 μM) and 0.4 equivalent (14 μM), respectively (insets of Fig. 1). The limit of detection (LOD) of SQ1 was determined to be 0.211 μM (211 nM) or 7.2 ppb (Fig. 2). Considering of permission of emission level (PEL) [13] of H_2S is 20 ppm, LOD of SQ1 suggests excellent applicability to the H_2S sensor.

For more quantitative study on the different sensitivities of three SQ dyes, we examined kinetic profiles of the reaction between the SQ dyes and H_2S. To determine the stoichiometry and binding constant of the SQ-H_2S complex, Benesi-Hildebrand (BH) plot was used [14]. As shown in Fig. 3, all SQ dyes exhibited a linear relationship between $1 / (A - A_0)$ and $1 / [H_2S]$ indicating 1:1 binding stoichiometry. The association constant values were calculated using equation given as follows:

$$\frac{1}{A-A_0} = \frac{1}{K_{ass}(A_{max}-A_0)[H_2S]} + \frac{1}{A_{max}-A_0}$$

where A_0 is the absorbance of SQ, A is the absorbance obtained with addition of the H_2S, A_{max} is the absorbance obtained with an excess amount of hydrogen sulfide, K_{ass} is the association constant (M^{-1}), and $[H_2S]$ is the concentration of the added hydrogen sulfide. From the linear relationship in the plot, the K_{ass}'s were calculated to be

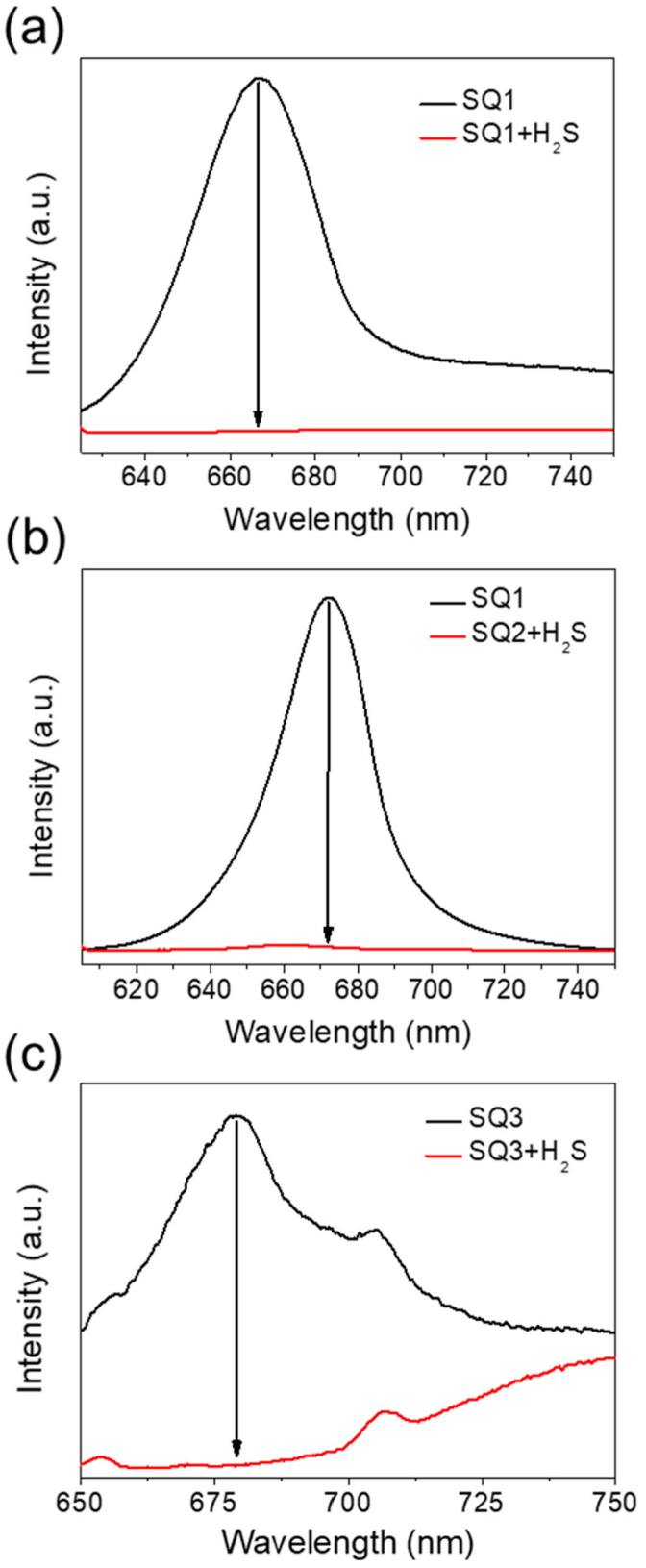

Fig. 6. Photoluminescence spectra for (a) **SQ1** (1.0×10^{-4} M), (b) **SQ2** (2.5×10^{-4} M), (c) **SQ3** (5.0×10^{-5} M) upon addition of H2S.

1.11×10^6 (at 649 nm), 2.27×10^5 (at 650 nm), and 9.66×10^4 M^{-1} (at 663 nm) for the **SQ1**, **SQ2** and **SQ3**, respectively, which indicates the 1:1 association between SQ dyes and H_2S. These results imply that superior reactivity of **SQ1** with H_2S originated from the

corresponding higher binding constant compared to those of **SQ2** and **SQ3**.

Then, to investigate the origin of higher K_{ass} of **SQ1**, we explored the H_2S sensing mechanism of the SQ dyes. Rapid decrease of absorption intensity of **SQ1** shown in Fig. 1 suggests a high initial reaction rate of the nucleophilic attack of the H_2S on the four-atoms ring of SQ1. For detailed characterization of the reaction, we carried out NMR studies. Fig. 4 compares ^{1}H NMR spectra of **SQ1** solution before and after addition of H_2S. With the addition of H_2S, the peak from aromatic protons (8.41 ppm) showed up-field shift and separation into two peaks. These result indicate that electron deficient central cyclobutene ring of the SQ dyes is susceptible to nucleophilic attack which can break the conjugation and subsequently induce color bleaching of the dyes, which is consistent with previous reports [15]. Fig. 5 shows energy levels and electron distribution for frontier molecular orbitals of **SQ1** obtained by density functional theory (DFT)-based quantum chemical calculations which were performed through Perdew-Burke-Ernzerhof (PBE) function of generalized gradient approximation (GGA) level with double numeric states in frontier molecular orbitals. After reaction with H_2S at the proposed carbon of cyclobutene, bandgap (Eg) of SQ1 changed from 1.272 to 2.613 eV while calculated oscillator strength of SQ1 at 600 nm significantly decreased after the reaction, which supports the proposed reaction mechanism. Furthermore, as presented in Fig. 6, photoluminescence (PL) emission quenching also support the conjugation break of the SQ dyes when exposed to H_2S.

Considering that the reaction site is located at the carbon of the cyclobutene of the SQ dyes, it can be inferred that lower reactivity of **SQ2** and **SQ3** compared to **SQ1** originated from larger steric hindrance effects of hydroxyl and methyl groups in **SQ2** and **SQ3**, respectively. The calculated distance between **SQ1** and HS (2.322 Å) is much shorter than those for **SQ2** (3.251 Å) and **SQ3** (4.540 Å), which is in accordance with the different relative reactivities (K_{ass} values) obtained from the experimental results (Fig. 7).

Selectivity to the specific analyte is a key requirement for efficient chemosensor function. To evaluate the selectivity of **SQ1**, various analytes including H_2S, common anionic species such as F^-, Cl^-, I^-, HPO_4^{2-}, PO_4^{3-}, NO_2^- and N_3^- and reactive oxygen/nitrogen species (ROS/RNS) H_2O_2 were added to the **SQ1** solution (2.5×10^{-4} M in DMSO:H_2O = 4:1) and their optical property changes were recorded. Excellent selectivity of SQ1 to H_2S is presented in Fig. 8 by demonstrating UV–Vis absorption spectral change and ratio of absorbance changes

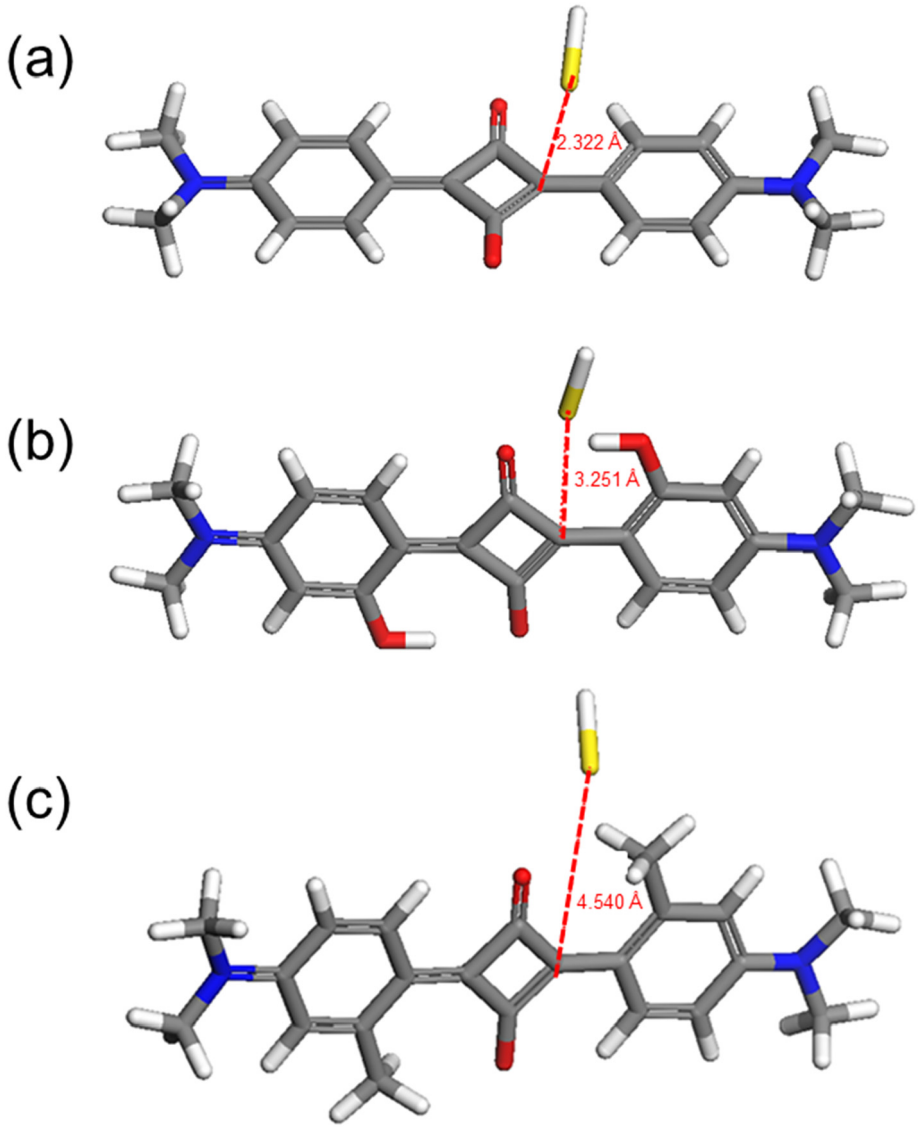

Fig. 7. Calculated distances between H_2S and SQ dyes.

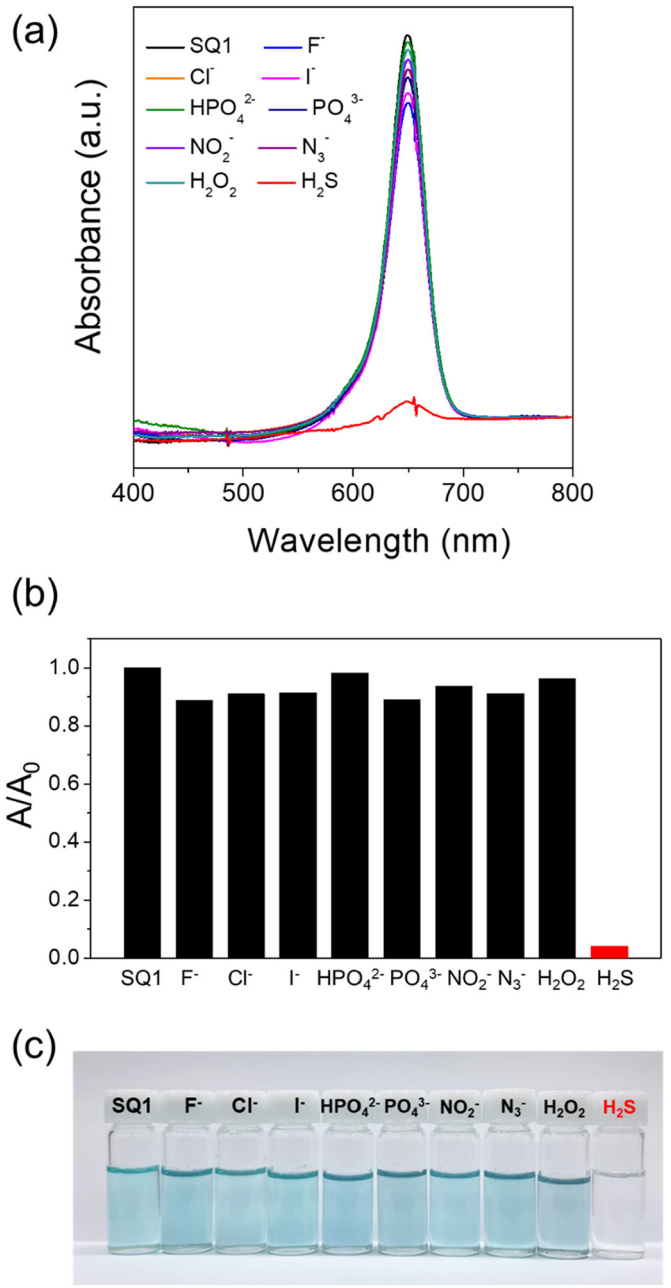

Fig. 8. (a) UV–Vis absorption spectrum changes in response to various anion analytes, (b) comparison of absorption ratio for various anions in **SQ1** (A and A_0 are the absorbance in the presence and the absence of anions at 649 nm, respectively), and (c) photographs showing selective colorimetric change of SQ1 in response to the various anions.

of **SQ1** to different analytes. As shown in Fig. 8, when 1 equivalent of different anions were added into **SQ1** solution, addition of H_2S only exhibited naked-eye-discernable color change by UV–Vis spectral changes while addition of other anions did not have significant effect on the absorption spectrum and color changes of **SQ1** solution. Furthermore, upon addition of different nucleophiles (sodium sulfide (Na_2S), thiophenol (PhSH), and glutathione (GSH)) to **SQ1** solution, color changes was observed from Na_2S due to the H_2S generation and PhSH addition, as shown in Fig. S3.

Finally, in order to demonstrate the practical application of **SQ1** for H_2S detection, we investigated their detection capability in solid state and in dyed fabric. Solution of **SQ1** (20 ml, 5.0×10^{-4} M) was added to silica (230–400 mesh, 3 g, white), stirred for 1 min, and dried to prepare blue silica. When the SQ1-silica was exposed to H_2S (2 ml, 1.0×10^{-4} M), it showed marked color change to light blue with ultra-fast detection speed (<1.0 s) with ambient stability over 10 days, as shown in Fig. 9a and Fig. S4. In addition, we also investigated H_2S detection properties of solid **SQ1** by using **SQ1**-dyed fabric as shown in Fig. 9b. **SQ1**-dyed fabric were prepared by dipping polyethylene terephthalate (PET) textile into **SQ1** solution. After drying, the dyed fabric were exposed to a H_2S gas with a total flow rate of 1000 sccm (dry air:H_2S (1000 ppm) = 1:1) in the chamber. Noticeable color change from blue to colorless was clearly observed. Rapid and naked-eye-based colorimetric H_2S sensing capability of **SQ1** in solid states suggest the potential applicability to cheap, simple but very effective practical H_2S sensors such as optical solid chemosensors. The color change was measured by applying the commonly used Commission Internationale de L'Eclairage (CIE) Lab standard among various color quantifications. The changes in the CIE L*, a*, b*, and chroma (C) values, and the hue angle (H), are shown in Table 1. The three coordinates of the CIE Lab represent the lightness of the color (L* = 0 yields black and L* = 100 indicates diffuse white; specular white may be higher), its position between red/magenta and green (a*, negative values indicate green, while positive values indicate magenta), and its position between yellow and blue (b*, negative values indicate blue and positive values indicate yellow). From the coordinate values, the color change (ΔEab) was calculated using equation given as follows:

$$\Delta Eab = \sqrt{(\Delta L^*)^2 + (\Delta a^*)^2 + (\Delta b^*)^2}$$

In general, when the color change value is 5 or higher, observers can recognize two distinctive colors [16]. The dyed fabric exhibited a color difference value of 6.69, indicating that before and after gas exposure, the color of the fabric is perceptible.

4. Conclusion

In summary, we synthesized squarylium-based chromogenic H_2S chemosensors (**SQ1**, **SQ2**, and **SQ3**), systemically characterized the detection performances, and elucidated the sensing mechanism. **SQ1** exhibited naked-eye-discernable and rapid colorimetric changes when exposed to H_2S with detection limit of 7.2 ppb. **SQ1** featured high selectivity for H_2S detection over other relevant anions and nucleophiles. In addition to the solution environment, versatile detection capability of H_2S in solid state such as **SQ1**-coated silica and **SQ1**-dyed fabric suggests the simple, low-cost, and practical applications of **SQ1** to the effective H_2S chemosensors.

CRediT authorship contribution statement

Ha Lim Noh: Investigation. **Byeong M. Oh:** Investigation. **Young Ki Park:** Investigation. **Hye W. Chun:** Investigation. **Junyeop Lee:** Investigation. **Jae Keon Kim:** Investigation. **Jian Zheng:** Investigation. **Daewoong Jung:** Formal analysis, Writing - review & editing. **Woosung Lee:** Formal analysis, Writing - review & editing. **Jong H. Kim:** Conceptualization, Methodology, Supervision, Writing - original draft.

Declaration of competing interest

The authors declare that they have no known competing financial interests or personal relationships that could have appeared to influence the work reported in this paper.

Acknowledgement

This work was supported by Basic Science Research Program through the National Research Foundation of Korea (NRF) funded by the Ministry of Education (NRF-2018R1D1A1B07047645). This study was also supported by a grant from Priority Research Centers Program (2019R1A6A1A11051471) funded by the NRF. This study has been

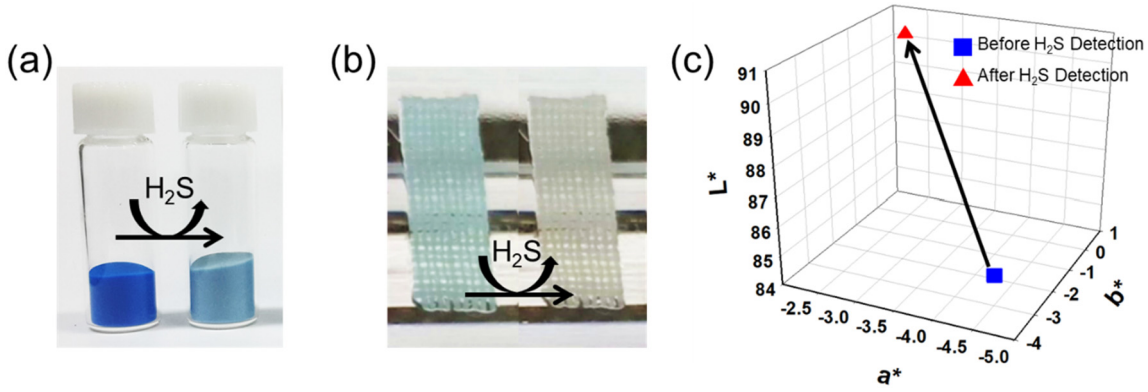

Fig. 9. Detection of H2S from (a) SQ1 in silica and (b) SQ1-dyed fabric, and (c) the CIE Lab coordinate value (L, a, b) change of the **SQ1**-dyed fabric after H_2S gas detection.

Table 1
Color values of **SQ1** on PET fabric.

Condition	L*	a*	b*	C	H	ΔE_{ab}
Before H_2S	85.24	−4.55	−3.21	5.57	215.18	6.69
After H_2S	90.27	−2.30	0.58	2.37	165.83	

conducted with the support of the Korea Institute of Industrial Technology (kitech EO-19-0052).

References

[1] a) C.-C. Lien, J.-L. Lin, C.-H. Ting, Water scrubbing for removal of hydrogen sulfide (H_2S) Inbiogas from hog farms, J. Agric. Chem. Environ. 3 (2014) 1–6;
b K.Y. Kim, H.J. Ko, H.T. Kim, Y.S. Kim, Y.M. Roh, C.M. Lee, C.N. Kim, Quantification of ammonia and hydrogen sulfide emitted from pig buildings in Korea, J. Environ. Manag. 88 (2008) 195–202;
c G. Gerasimon, S. Bennett, J. Musser, J. Rinard, Acute hydrogen sulfide poisoning in a dairy farmer, Clin. Toxicol. 45 (2007) 420–423;
d R.G. Hendrickson, A. Chang, R.J. Hamilton, Co-worker fatalities from hydrogen sulfide, Am. J. Ind. Med. 45 (2004) 346–350.

[2] a) G. Zagli, R. Patacchini, M. Trevisani, R. Abbate, S. Cinotti, G.F. Gensini, G. Masotti, P. Geppetti, Hydrogen sulfide inhibits human platelet aggregation, Eur. J. Pharmacol. 559 (2007) 65–68;
b) T.L. Guidotti, Hydrogen sulfide: advances in understanding human toxicity, Int. J. Toxicol. 29 (2010) 569–581.

[3] a) S. Rezaei, A. Tavana, J.A. Sawada, L. Wu, A.S.M. Junaid, S.M. Kuznicki, Novel copper-exchanged titanosilicate adsorbent for low temperature H_2S removal, Ind. Eng. Chem. Res. 51 (2012) 12430–12434;
b) A. Kulprathipanja, G.O. Alptekin, J.L. Falconer, J.D. Way, Pd and Pd–Cu membranes: inhibition of H_2 permeation by H_2S, J. Membr. Sci. 254 (2005) 49–62.

[4] K. Eto, T. Asada, K. Arima, T. Makifuchi, H. Kimura, Brain hydrogen sulfide is severely decreased in Alzheimer's disease, Biochem. Biophys. Res. Commun. 293 (2002) 1485–1488.

[5] a) J.R. Stetter, J.M. Sedlak, K.F. Blurton, Electrochemical gas chromatographic detection of hydrogen sulfide at PPM and PPB levels, J. Chromatogr. Sci. 15 (1977) 125–128;
b) A. Bagreev, T.J. Bandosz, Study of hydrogen sulfide adsorption on activated carbons using inverse gas chromatography at infinite dilution, J. Phys. Chem. B 104 (2000) 8841–8847;
c) J. Radford-Knoery, G.A. Cutter, Determination of carbonyl sulfide and hydrogen sulfide species in natural waters using specialized collection procedures and gas chromatography with flame photometric detection, Anal. Chem. 65 (1993) 976–982.

[6] a) J. Gong, Q. Chen, M.-R. Lian, N.-C. Liu, R.G. Stevenson, Fatos Adami, Micromachined nanocrystalline silver doped SnO_2 H_2S sensor, Sens. Actuators B Chem. 114 (2006) 32–39;
b) B. Spilker, J. Randhahn, H. Grabow, H. Beikirch, P. Jeroschewski, New electrochemical sensor for the detection of hydrogen sulfide and other redox active species, J. Electroanal. Chem. 612 (2008) 121–130.

[7] a) F. Hou, L. Huang, P. Xi, J. Cheng, X. Zhao, G. Xie, Y. Shi, F. Cheng, X. Yao, D. Bai, Z. Zeng, A retrievable and highly selective fluorescent probe for monitoring sulfide and imaging in living cells, Inorg. Chem. 51 (2012) 2454–2460;
b) R. Kaushik, P. Kumar, A. Ghosh, N. Gupta, D. Kaur, S. Arora, D.A. Jose, Alizarin red S–zinc(II) fluorescent ensemble for selective detection of hydrogen sulphide and assay with an H_2S donor, RSC Adv. 5 (2015) 79309–79316;
c) R. Kaushik, A. Singh, A. Ghosh, D.A. Jose, Selective colorimetric sensor for the detection of Hg^{2+} and H_2S in aqueous medium and waste water samples, ChemistrySelect. 1 (2016) 1533–1540.

[8] M. Colon, J.L. Todolí, M. Hidalgo, M. Iglesias, Development of novel and sensitive methods for the determination of sulfide in aqueous samples by hydrogen sulfide generation-inductively coupled plasma-atomic emission spectroscopy, Anal. Chim. Acta 609 (2008) 160–168.

[9] a) D.-W. Li, L.-L. Qu, K. Hu, Y.-T. Long, H. Tian, Monitoring of endogenous hydrogen sulfide in living cells using surface-enhanced Raman scattering, Angew. Chem. Int. Ed. 54 (2015) 12758–12761;
b) K. Lewin, J.N. Walsh, D.L. Miles, Determination of dissolved sulphide in groundwaters by inductively coupled plasma atomic emission spectrometry, J. Anal. At. Spectrom. 2 (1987) 249–250.

[10] V.S. Lin, C.J. Chang, Fluorescent probes for sensing and imaging biological hydrogen sulfide, Curr. Opin. Chem. Biol. 16 (2012) 595–601.

[11] a) T. Maeda, H. Nakao, H. Kito, H. Ichinose, S. Yagi, H. Nakazumi, Far-red absorbing squarylium dyes with terminally connected electron-accepting units for organic dye-sensitized solar cells, Dyes Pigments 90 (2011) 275–283;
b) J.-S. Bae, S.-Y. Gwon, Y.-A. Son, S.-H. Kim, A benzothiazole-based semisquarylium dye suitable for highly selective Hg^{2+} sensing in aqueous media, Dyes Pigments 83 (2009) 324–327;
c) C.W. Dirk, W.C. Herndon, F. Cervantes-Lee, H. Selnau, S. Martinez, P. Kalamegham, A. Tan, G. Campos, M. Velez, J. Zyss, I. Ledoux, L.-T. Cheng, Squarylium dyes: structural factors pertaining to the negative third-order nonlinear optical response, J. Am. Chem. Soc. 117 (1995) 2214–2225.

[12] a) S. Ding, W. Feng, G. Feng, Rapid and highly selective detection of H_2S by nitrobenzofurazan (NBD) ether-based fluorescent probes with an aldehyde group, Sens. Actuators B Chem. 238 (2017) 619–625;
b) J. Hong, E. Zhou, S. Gong, G. Feng, A red to near-infrared fluorescent probe featuring a super large Stokes shift for light-up detection of endogenous H_2S, Dyes Pigments 160 (2019) 787–793.

[13] Occupational Safety and Health Administration (OSHA) Permissible Exposure Limits (PELS) from 29 CFR 1910.1000 Z-2 Table.

[14] A.K. TG, V. Tekuri, M. Mohan, D.R. Trivedi, Selective colorimetric chemosensor for the detection of Hg^{2+} and arsenite ions using Isatin based Schiff's bases; DFT studies and applications in test strips, Sens. Actuators B Chem. 284 (2019) 271–280.

[15] a) I.-S. Shin, S.-Y. Gwon, S.-H. Kim, Chromogenic sensing of biological thiols using squarylium dye, Spectrochim. Acta A 120 (2014) 642–645;
b) T. Liu, F. Huo, C. Yin, J. Li, L. Niu, A highly selective fluorescence sensor for cysteine/homocysteine and its application in bioimaging, RSC Adv. 5 (2015) 28713–28716;
c) J.V. Ros-Lis, B. García, D. Jiménez, R. Martínez-Máñez, F. Sancenón, J. Soto, F. Gonzalvo, M.C. Valldecabres, Squaraines as fluoro–chromogenic probes for thiol-containing compounds and their application to the detection of biorelevant thiols, J. Am. Chem. Soc. 126 (2004) 4064–4065;
d) J. Fan, Z. Wang, H. Zhu, N. Fu, A fast response squaraine-based colorimetric probe for detection of thiols in physiological conditions, Sens. Actuators B Chem. 188 (2013) 886–893.

[16] W.S. Mokrzycki, M. Tatol, Colour difference Δ E-A survey, Mach. Graph. Vis. 20 (4) (2011) 383–411.